Cellular and Molecular Biology
E-ISSN : 1165-158X / P-ISSN : 0145-5680
www.cellmolbiol.org

miR-19a-3p affected ox-LDL-induced SDC-1/TGF-β1/Smad3 pathway in atherosclerosis

Qiao Jin[1, 2 #], Yiming Deng[1,3#], Liang Li[1], Ran Chen[1*], Luping Jiang[1*]

[1] The Changsha central Affiliated Hospital, Department of Cardiovascular Medicine, Hengyang Medical School, University of South China, Changsha, Hunan, 410004, China
[2] Department of Cardiovascular Medicine, The Third Xiangya Hospital of Central South University, Changsha 410013, Hunan Province, China
[3] Graduate School , Hunan University of Chinese Medicine, Changsha, Hunan, 410208, China

[#]Qiao Jin and Yiming Deng contributed equally to this paper. They are co-first authors.

ARTICLE INFO

Original paper

Article history:
Received: January 9, 2023
Accepted: March 14, 2023
Published: March 31, 2023

Keywords:

TALNEC2, miR-19a-3p, JNK, cerebral infarction, cell viability, inflammation, apoptosis

ABSTRACT

Syndecan-1 (SDC-1) was a critical membrane proteoglycan and an important component of the glycocalyx in endothelial cells, but its role in atherosclerosis remains unknown. This study attempted to investigate the role of SDC-1 in atherosclerotic-related endothelial cell injury. Bioinformatics analyzed the differential miRNAs between atherosclerosis and healthy. Subjects with coronary atherosclerosis, which were diagnosed with intravascular atherosclerosis (IVUS), were enrolled as non-vulnerable plaque and vulnerable plaque in Changsha Central Hospital. Human aortic endothelial cells (HAECs) were induced by oxidized low-density lipoprotein (ox-LDL) to construct an *in vitro* model. A dual luciferase reporter assay was applied to analyze the target between miR-19a-3p and SDC-1. The cell proliferation and apoptosis were detected by CCK8 and flow cytometry, respectively. SDC-1 and cholesterol efflux was determined by ELISA. The expression of ATP-binding cassette (ABC) transports A1 (ABCA1), miR-19a-3p, ABCG1 and SDC-1 genes were detected by RT-qPCR. The expressions of SDC-1, ABCA1, ABCG1, TGF-β1, Smad3 and p-Smad3 proteins were detected by western blot. Our results found that miR-19a-3p was down-regulated in atherosclerosis. ox-LDL decreased miR-19a-3p expression, increased cholesterol efflux and the expression of ABCA1, ABCG1 and SDC-1 in HAECs. Vulnerable plaque tissues in patients with coronary atherosclerosis showed palpable fibrous necrosis and calcification with elevated blood SDC-1 levels. miR-19a-3p could bind to SDC-1. Overexpression of miR-19a-3p promoted cell proliferation, inhibited apoptosis and cholesterol efflux, down-regulated the expression of SDC-1, ABCA1, ABCG1, TGF-β1 and p-Smad3 proteins in ox-LDL-induced HAECs. In conclusion, miR-19a-3p targeting SDC-1 inhibited the ox-LDL-induced activation of the TGF-β1/Smad3 pathway in HAECs.

Doi: http://dx.doi.org/10.14715/cmb/2023.69.3.10

Introduction

Atherosclerosis was the main cause of vascular diseases worldwide, and its main clinical manifestations included ischemic heart disease, ischemic stroke, and peripheral artery disease (1). The walls of blood vessels atherosclerosis were considered to be the result of the accumulation of lipid passive (2). The pathological process was characterized by intimal infiltration and modification of plasma-derived lipoproteins and uptake by macrophages, which were followed by the formation of lipid-filled foam cells and led to the formation of atherosclerotic lesions (3). Vulnerable plaque refers to the late lesion of the necrotic core formed by secondary necrotic macrophage and foam cell accumulation, which were caused by defective endocytosis and inadequate inflammatory response (3). Plaques that did not cause significant hemodynamic stenosis might also cause cardiac events, such as plaque rupture associated with thin caps, lipid-rich plaques, plaque erosion, calcified nodules and plaque local vascular functional lesions (4). Clinical studies proved that miRNA expression profiles derived from atherosclerotic plaque materials were associated with the stability of coronary artery disease (5), which might contribute to the search for new therapeutic strategies for cardiovascular disease.

Changes in the hemodynamics of the vascular system lead to changes in miRNA expression (6). miRNA plays an important role in gene regulation by pairing with the mRNA of protein-coding genes to fine-tune post-transcriptional inhibition (6). Animal studies have shown that dynamic changes in miRNAs expression profiles in plasma, platelets and platelet-derived microbubbles were involved in the development of atherosclerosis (7). miR-19a-3p was known to be one of the miRNAs induced by high shear stress that mediated atherosclerosis (6, 8). Silencing miR-19a-3p inhibited the proliferation and invasion of atherosclerotic vascular endothelial cells (9). It is known that miR-19a-3p/SDC-1 inhibited the JAK1/STAT3 signaling pathway activation, which ameliorated cerebral ischemic injury (10). However, the mechanism of miR-19a-3p-mediated SDC-1 expression in the pathogenesis of coronary atherosclerosis was still unknown.

SDC-1 was a critical membrane proteoglycan that has been reported to be involved in the regulation of tissue re-

* Corresponding author. Email: 2018051255@usc.edu.cn ; Email: 2018050067@usc.edu.cn

pair and chronic injury response events, such as cell-substrate interactions, matrix remodeling, and cell migration (11). Studies of hemodynamics and fluid shear stress suggested that SDC-1 was involved in controlling mechanical sensing and flow-mediated phenotypic regulation of endothelial cells (12). Lower SDC-1 levels were associated with a higher prevalence of lipid-rich plaques in patients with coronary artery diseases, which suggested a link between endodermis glycocalyces damage and the development of lipid-rich plaques (13). During atherosclerotic disease, the damage and degradation of the endodermal calyx were accompanied by the shedding of SDC-1 into the bloodstream, which could directly reflect the health of the endodermal calyx and blood vessels (14). Therefore, exploring the mechanism of SDC-1 in the vascular endothelium of atherosclerotic diseases might contribute to the development of potential therapies.

Plasma ox-LDL was significantly correlated with carotid plaque, and ox-LDL in the vulnerable plaque group was significantly higher than that in the stable plaque group (15). Rapid deposition of ox-LDL could lead to rapid plaque progression, increased necrotic core, and decreased stability due to the breakdown of the endothelial barrier in advanced plaques (16). TGF-β1 was induced by oxidized low-density lipoprotein (ox-LDL) and contributed to atherosclerotic-associated vascular endothelial cell damage (17). TGF-β1/Smad3 signaling pathway ubiquitously is widely found in various tissues and cells and is also associated with the development of cardiovascular diseases (18), such as atherosclerosis complicated with hydrocephalus (19). It was known that ox-LDL induced matrix accumulation through TGF-β/Smad3 signaling in mesangial cells (20). However, the role of SDC-1 and TGFβ1/Smad3 in ox-LDL-induced endothelial cell injury remains unknown. This study intends to establish the ox-LDL-induced injury model of HAECs to explore the role of miR-19a-3p-mediated SDC-1 in atherosclerotic diseases (21), in order to provide a new strategy for the treatment of coronary atherosclerosis.

Materials and Methods

Bioinformatics analysis

The GSE153813 miRNAs data was used in this study. All data were normalized. The data contained five atherosclerosis and three controls. Limma package (R language) was applied for inter-group difference analysis with cutoff ($|logFC|>log_2 1.5$ & $p<0.05$). The heatmap was applied to show the different analysis results of miRNAs. The box plot was applied to show the expression of miR-19a-3p. TargetScan was applied to predict the binding site of miR-19a-3p to SDC-1 (22).

Cell experiment and grouping

HAECs were purchased from Procell (CP-H080, Procell) and cultured with an incubator containing 10 % FBS, 1 % penicillin G, 1 % streptomycin and 1 % endothelial growth factor at 37°C, 5 % CO_2 and saturated humidity. Logarithmic growing cells were divided into the Control group (PBS), ox-LDL group (50 mg/L ox-LDL, IO1300, Solarbio), NC mimics group (transfected with no load plasmid + 50 mg/L ox-LDL, HG-MI029489, Honorgene) and miR-19a-3p mimics group (transfected with miR-19a-3p overexpressed plasmid + 50 mg/L ox-LDL, HG-MI029489, Honorgene).

Clinical subject

Patients with coronary atherosclerosis, which were diagnosed with intravascular atherosclerosis (IVUS) in Changsha Central Hospital, were enrolled as the non-vulnerable plaque group and vulnerable plaque group, 10 patients/group, respectively (23). IVUS was used to generate three-dimensional elastic maps to evaluate the mechanical properties of atherosclerotic plaques (23-25). The baseline characteristics of non-vulnerable plaque and vulnerable plaque subjects were shown in Table 1. Coronary blood was extracted from non-vulnerable plaque and vulnerable plaque subjects using catheters and stored after centrifugation (26). Subjects were excluded as follows: renal insufficiency, recently infected persons, cardiac arrest or circulatory shock (systolic blood pressure below 90 mmHg) at the prehospital stage or admission, suspected infections, chronic diseases such as heart failure, cirrhosis, and tumors. Informed consent was also signed by all subjects and their families. Ethical approval was obtained from the Ethics Committee of Nanhua University Affiliated Changsha Central Hospital (201812).

Table 1. Baseline characteristics of non-vulnerable plaque and vulnerable plaque subjects.

Groups	non-vulnerable plaque group (n=15)	vulnerable plaque group (n=15)	*P*-value
Age (years)	61.50±3.23	63.70±5.33	0.965
Sex (male, %)	86.66	86.66	-
BMI (kg/m2)	21.63±1.68	23.31±2.11	0.341
SBP (mmHg)	118.50±5.61	121.20±18.3	0.752
DBP (mmHg)	77.40±3.82	75.60±8.31	0.496
ALT (U/L)	29.34±7.22	28.02±9.42	0.614
CRE (μmol/L)	74.26±6.14	82.33±17.56	0.244
FBG (μmol/L)	5.64±0.75	5.98±1.17	0.237
TC	4.85±0.21	4.24±0.56	0.047
TG (mmol/L)	0.92±0.12	1.11±0.39	0.324
HDL-C (mmol/L)	1.28±0.12	1.09±0.17	0.033
LDL-C (mmol/L)	2.91±0.52	3.74±0.87	0.029

BMI, Body Mass Index. SBP, Systolic Blood Pressure. DBP, Diastolic Blood Pressure. ALT, Alanine transaminase. CRE, Creatinine. FBG, Fasting Blood Glucose. TC, Total cholesterol. TG, Triacylglycerol. HDL-C, high-density lipoprotein cholesterol. LDL-C, low-density lipoprotein cholesterol. The data were analyzed by Student's t-test.

Construction of HAECs overexpressing miR-19a-3p

The no-loaded overexpressed plasmids and miR-19a-3p overexpressed plasmids were defrosted on ice. Serum-free DMEM medium (95 μL) was added to each sterile centrifuge tube. Then, 2.5 μg no-loaded overexpressed plasmid and 5 μL Lip2000 (Invitrogen) were added to the centrifuge tubes, respectively. miR-19a-3p overexpressed plasmid (HG-MI029489, Honorgene) was also added into the corresponding centrifuge tubes according to this method. The reagents were gently mixed and incubated at room temperature for 5 min. Finally, the mixture was evenly added to the well to be transfected and mixed. After 6 h culture in a 37°C incubator, the fresh complete culture medium was changed.

Cell Counting Kit-8 (CCK8)

The cells were digested, counted and inoculated into a 96-well plate (0030730119, Eppendorf) with a density of 5×10^3 cells/well, 100 μL/well. Each group was equipped with 3 multiple holes. After culture and adhesion, the CCK8 solution (10:1, NU679, DOJINDO) was prepared by a complete medium, which was added to each well. Then, the Bio-Tek microplate (MB-530, Heals) was used to analyze the absorbance value at 450 nm.

Flow cytometry

The cells were centrifuged at 1500 rpm for 5 min to collect. Annexin V-APC apoptosis detection kit (KGA1019, Nanjing KeyGen Biotech Co., Ltd.) was used. A binding buffer (500 μL) was added to suspension cells. Annexin V-APC (5 μL) and 5 μL propidium Iodide were added to cells and mixed, respectively. The cells were incubated far away from light. Flow cytometry (A00-1-1102, Beckman) was used to detect apoptosis.

Enzyme-linked immunosorbent assay (ELISA)

The coronary blood samples were placed at room temperature for 2 h and centrifuged at 1000 g for 15 min to collect the supernatant for detection. The supernatant of the cell was also centrifuged and collected for detection. The SDC-1 levels were detected by using the SDC-1 detection kit (CSB-E14983H, CUSABIO) and a multifunctional ELISA analyzer (MB-530, Heals).

Cholesterol efflux

A cholesterol efflux fluorometric assay kit (K582-100, Biovision Incorporated) was used to detect cholesterol efflux. Briefly, 1×10^5 HAECs were inoculated into each well of a 96-well plate and incubated for 2 h. Next, fluorescently labeled cholesterol was added to each well and incubated for 15 h before the supply of ox-LDL. The supernatant was collected, and its fluorescence was measured. The supernatant of lysed HAECs was transferred, and their fluorescence was measured. Cholesterol efflux was calculated by the formula: Cholesterol efflux (%) = RFU of Supernatant/(RFU of Cell Lysate + RFU of Supernatant).

Dual-luciferase reporter assay

The 293T cells were purchased from HonorGene (HG-NC002, HonorGene) and cultured with a 24-well plate. The pHG-MirTarget-SDC-1-3U and pHG-MirTarget-SDC-1 MUT-3U were used for transfection-level plasmid extraction. A dual luciferase reporter assay kit (E1910, Promega) was applied to dual luciferase reporter assay. Cells were transfected by Lip2000 transfection reagent (Invitrogen), miR-19a-3p mimics (HG-MI029489, Honorgene) and miRNA NC (HG-MI029489, Honorgene), respectively. The specific groups were as follows: NC mimics + SDC-1 WT group, miR-19a-3p mimics + SDC-1 WT group, NC mimics + SDC-1 Mut group, miR-19a-3p mimics + SDC-1 Mut group. Cells in NC mimics + SDC-1 WT group were co-transfected phG-mirtarget-SDC-1-3U large plasmid and miRNA NC. Cells in miR-19a-3p mimics + SDC-1 WT group were co-transfected phG-mirtarget-SDC-1-3U large plasmid and miR-19a-3p mimics. Cells in NC mimics + SDC-1 Mut group were co-transfected phG-mirtarget-SDC-1 MUT-3U large plasmid and miRNA NC. Cells in miR-19a-3p mimics + SDC-1 Mut group were co-transfected phG-mirtarget-SDC-1 MUT-3U large plasmid and miR-19a-3p mimics. The final concentration of the cotransfection reagent in each group was 50 nM. The cells were cleaned twice with 1×PBS to remove all the cleaning fluid. Then, the corresponding volume of 1×PLB lysate was added. The culture plates were gently shaken for 15 min to lysate the cells. Cell lysate (20 μL) was added into a 1.5 mL centrifuge tube, followed by 100 μL of LARII solution. The mixture was put into a luminescence detector (GloMax 20/20, Promega) to detect the luciferase activity of fireflies. Then, 100 μL Stop&Glo detection solution was added to stop the first luminescence and start the second luminescence at the same time. After the mixture, the luciferase activity of the sea kidney was detected by the luminescence detector (GloMax 20/20, Promega).

Real-time quantitative polymerase chain reaction (RT-qPCR)

Trizol (V900483, Sigma) was used to extract total RNA from the cells. The mRNA was used as a template to reverse transcription cDNA by using the mRNA reverse transcription kit (CW2569, Beijing, China). The expression of target genes was detected by the UltraSYBR Mixture (CW2601, Beijing, China) and fluorescence quantitative PCR instrument (PIKOREAL96, Thermo). The expression of SDC-1, ABCA1, ABCG1 and miR-19a-3p genes were calculated by the $2^{-\Delta\Delta Ct}$ algorithm with β-actin or U6 as internal parameters, respectively. Primer sequences of genes were shown in Table 2.

Western blot

Cells were collected and added with RIPA lysis buffer to extract the protein. BCA (Bicinchoninic acid) method was applied to extract and determine the protein concentration. A total of 200 μg protein samples were separated and transferred by 12 % SDS-PAGE and PVDF membrane, respectively. The primary antibodies included anti-SDC-1 (10593-1-AP, Proteintech), anti-ABCA1 (ab66217, Thermo Fisher), anti-ABCG1 (ab52617, Proteintech), anti-TGF-β1 (ab215715, Abcam), anti-p-Smad3 (ab52903, Abcam), anti-Smad3 (ab40854, Abcam) and anti-β-actin (66009-1-Ig, Proteintech). Then, it was conjugated with anti-IgG (SA00001-1, Proteintech) to incubate at 37°C for 90 min. Visualization and imaging analysis were analyzed by Millipore chemiluminescence and GE Healthcare software (Life Sciences), respectively.

Data statistics and analysis

GraphPad Prism 8.0 statistical software was used for the statistical analysis of data in this study. Normality and

Table 2. Primer sequences.

Gene	Primer sequences		Length
SDC-1	F	AGCTGAAAGGCCGGGAAC	154bp
	R	CGCTCTCTACTGCCGGATTC	
ABCA1	F	GTTAGGAAACCTGCTGCCCT	185bp
	R	ATGCCACACACAGGACGTAG	
ABCG1	F	TGTCTGATGGCCGCTTTCTC	110bp
	R	CTCTGGACACCACCTCATCCAC	
β-actin	F	ACCCTGAAGTACCCCATCGAG	224bp
	R	AGCACAGCCTGGATAGCAAC	
U6	F	CTCGCTTCGGCAGCACA	94bp
	R	AACGCTTCACGAATTTGCGT	
miR-19a-3p	GTGACAAATCTATGCAAAACTGA		

homogeneity of variance tests were performed first, which were consistent with normal distribution and homogeneity of variance. Statistical significance between two groups within experiments was determined by unpaired two-tailed Student's t-tests, while among more than two groups was determined by one-way ANOVA. Tukey's post-test was used for comparison. The measurement data were expressed as mean ± standard deviation. $P < 0.05$ indicated that the difference was statistically significant.

Results

miR-19a-3p was down-regulated in atherosclerosis and ox-LDL-induced HAECs

Heatmap showed the differential miRNAs between the atherosclerotic patients and healthy (Figure 1A). The expression of miR-19a-3p was lower in atherosclerosis than that in the healthy (Figure 1B). Compared with the Control group, ox-LDL induced the down-regulation of miR-19a-3p genes in HAECs (Figure 1C). The ox-LDL-induced apoptosis inhibited proliferation and increased cholesterol efflux in HAECs (Figure 1D-F). Compared with the control group, the ABCA1 and ABCG1 gene expressions were significantly increased in the ox-LDL group (Figure 3G). All the results proved that miR-19a-3p was down-regulated in atherosclerosis and ox-LDL-induced HAECs.

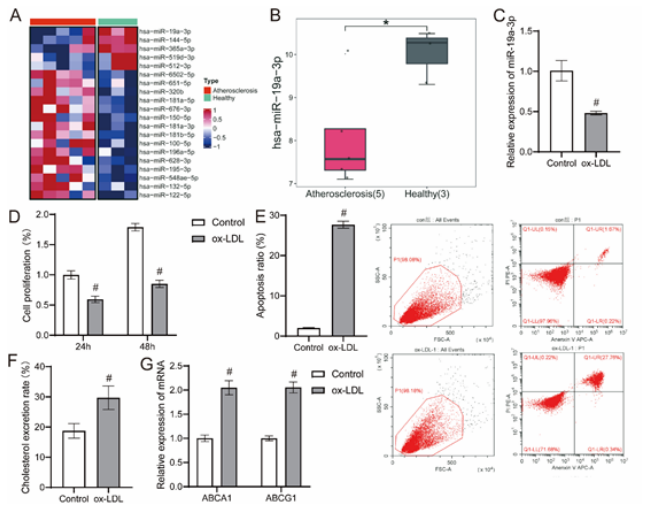

Figure 1. miR-19a-3p was down-regulated in atherosclerosis and ox-LDL-induced HAECs. (A) Heatmap was applied to show the differential miRNAs between the atherosclerotic and healthy groups. (B) Boxplot was applied to show the expression of miR-19a-3p. (C) The expression of miR-19a-3p was detected by RT-qPCR. (D) HAECs activity was detected by CCK-8. (E) Apoptosis of HAECs was detected by flow cytometry. (F) Cholesterol efflux was detected by Fluorometric assay. (G) The expression of ABCA1 and ABCG1 was detected by RT-qPCR. *P<0.05 vs. Healthy group; #P<0.05 vs. Control group.

SDC-1 levels were up-regulated in vulnerable plaque subjects and ox-LDL-induced HAECs

Compared with the control group, the SDC-1 gene and protein expressions were significantly increased in the ox-LDL group (Figure 2A-B). Coronary angiography combined with IVUS showed clearly fibrous necrosis and calcification in vulnerable plaque tissues of patients with coronary atherosclerosis (Figure 2C). Compared with the non-vulnerable plaque group, the levels of SDC-1 were significantly increased in the vulnerable plaque group (Figure 2D). These results suggested that the levels of SDC-1 in blood might be involved in the development of vulnerable plaque in atherosclerosis.

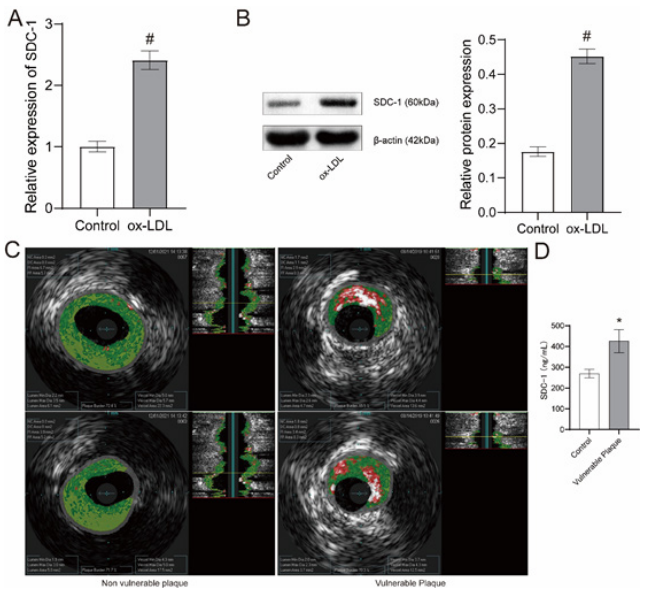

Figure 2. The SDC-1 levels were increased in the blood of subjects with vulnerable plaque. (A-B) The expression of SDC-1 was detected by RT-qPCR and western blot. (C) Representative IVUS images of non-vulnerable plaque and vulnerable plaque were observed. Blue represented fibrous plaques, white represented calcified plaques, and red represented the necrotic core of the plaque. (D) SDC-1 levels in coronary blood were detected by ELISA. *P<0.05 vs non-vulnerable plaque group, #P<0.05 vs. Control group.

miR-19a-3p targeted SDC-1

Bioinformatics analysis showed that miR-19a-3p and SDC-1 have binding sites (Figure 3A). Dual luciferase reporter assay demonstrated that compared with the NC mimics + SDC-1 WT group, the SDC-1 expression was significantly decreased in the miR-19a-3p mimics + SDC-1 WT group (Figure 3B). There was no significant change in SDC-1 expression between the NC mimics + SDC-1 Mut group and miR-19a-3p mimics + SDC-1 Mut group (Figure 3B). These results showed that miR-19a-3p could bind to SDC-1.

Overexpression of miR-19a-3p inhibited SDC-1 expression and cholesterol efflux in ox-LDL-induced HAECs

Overexpression of miR-19a-3p promoted the proliferation and inhibited apoptosis in ox-LDL-induced HAECs (Figure 4A-B). Overexpression of miR-19a-3p inhibited the expression of SDC-1, ABCA1 and ABCG1 in ox-LDL-induced HAECs (Figure 4C-D). Overexpression of miR-19a-3p inhibited ox-LDL-induced cholesterol efflux in HAECs (Figure 4E). These results suggested that overexpression of miR-19a-3p inhibited SDC-1 expression and improved the cholesterol efflux in ox-LDL-induced HAECs.

Up-regulation of miR-19a-3p inhibited the TGF-β1/Smad3 pathway in ox-LDL-induced HAECs

ox-LDL induced the increase of TGF-β1 and p-Smad3 proteins expression in HAECs (Figure 5). Overexpression of miR-19a-3p inhibited the TGF-β1 and p-Smad3 proteins expression in ox-LDL-induced HAECs (Figure 5). These results proved that up-regulation of miR-19a-3p inhibited the TGF-β1/Smad3 pathway in ox-LDL-induced HAECs.

Discussion

Atherosclerosis was also a lipoprotein-driven inflammatory disease that caused plaque formation in specific parts of the arterial tree (27). Syndecans were transmembrane heparin sulfate proteoglycans, which were involved in the regulation of cell growth, differentiation, adhesion, neuronal development and lipid metabolism (28). Animal studies have shown that SDC-1 signaling was weak in the normal aorta and that arterial injury-induced SDC-1 expression at mRNA and protein levels (29). Biomarkers have multiple clinical applications at multiple stages of diagnosis and treatment (30). Increased expression of SDC-1 and prevention of increased inflammation was observed in myocardial infarction (30). Our study proved that significant fibrous necrosis and calcification appeared in vulnerable plaque tissues of patients with coronary atherosclerosis, which was accompanied by elevated blood SDC-1 levels. Therefore, these studies proved that SDC-1 was involved in the pathological process of atherosclerotic

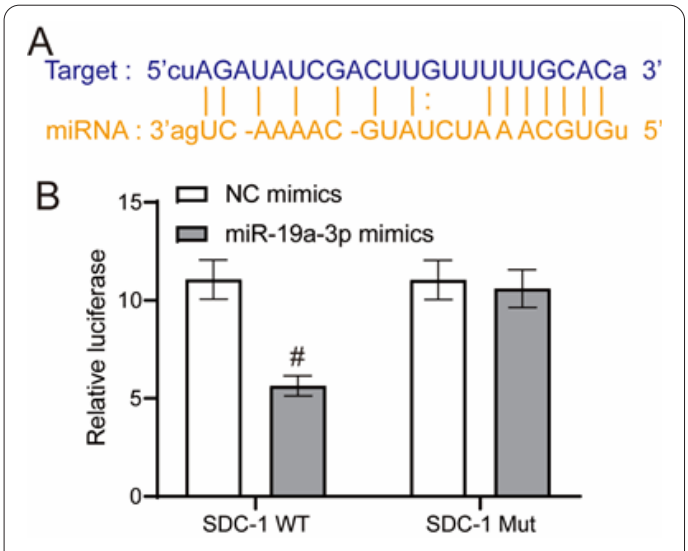

Figure 3. miR-19a-3p targeted SDC-1. (A) TargetScan predicted the binding site of miR-19a-3p to SDC-1. (B) Dual luciferase reporter assay showed that miR-19a-3p could bind to SDC-1. *P<0.05 vs. NC mimics + SDC-1 WT group. #P<0.05 vs. NC mimics group.

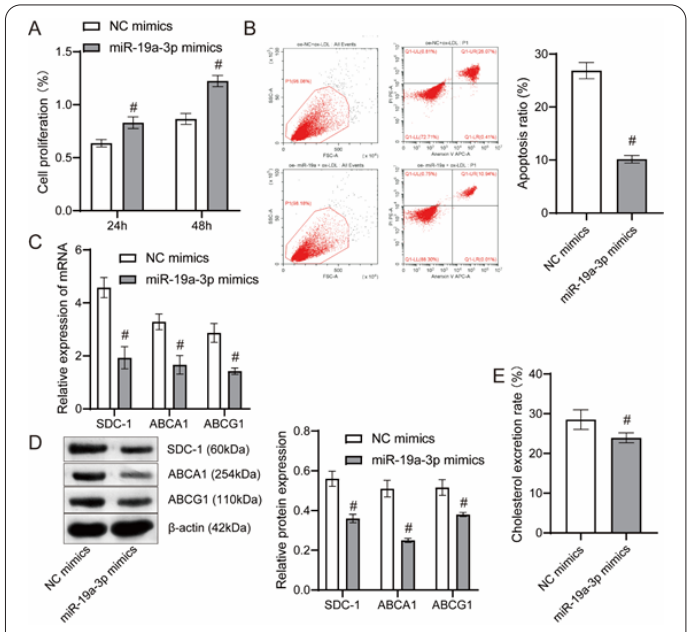

Figure 4. Overexpression of miR-19a-3p inhibited ox-LDL-induced HAECs damage and cholesterol efflux. (A) HAECs activity was detected by CCK-8. (B) Apoptosis of HAECs was detected by flow cytometry. (C-D) The expression of SDC-1, ABCA1 and ABCG1 was detected by RT-qPCR and western blot. (E) Cholesterol efflux was detected by a fluorometric assay. #P<0.05 vs. NC mimics group.

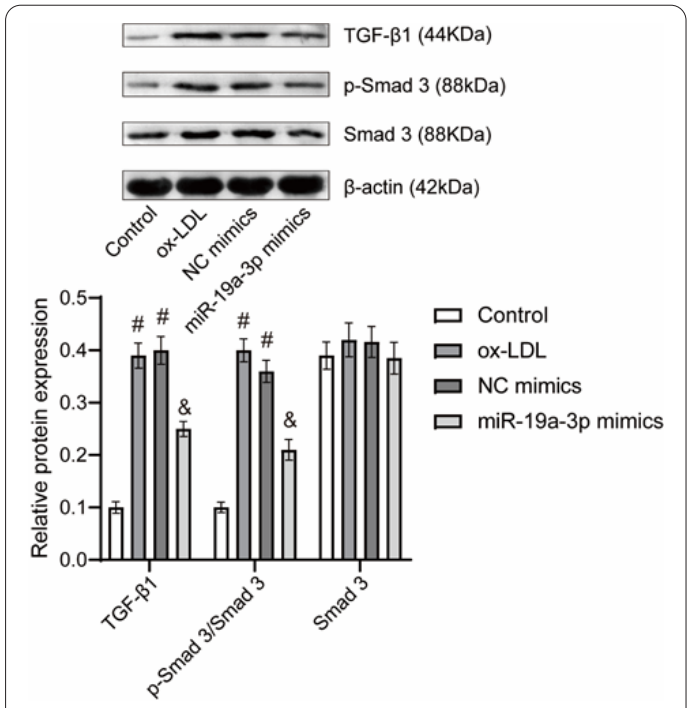

Figure 5. Overexpression of miR-19a-3p inhibited the TGF-β1/Smad3 pathway. The protein expression of TGF-β1, Smad3, and p-Smad3 was detected by western blot. #P<0.05 vs. Control group, &P<0.05 vs. NC mimics group.

plaques, which was urgent to further study the mechanism of SDC-1.

Atherosclerosis was a buildup of lipid plaques in the blood vessels, primarily due to endothelial damage caused by ox-LDL (31). ox-LDL played a central role in atherosclerosis by acting on a variety of cells via LOX-1, such as endothelial cells, macrophages, platelets, fibroblasts, and smooth muscle cells (32). We induced HAECs with ox-LDL and found an increase in cholesterol efflux, a decrease in miR-19a-3p expression, and an increase of ABCA1, ABCG1 and SDC-1 expression. SDC-1 was one of the major receptors for residual chylomicron absorption in the absence of LDL receptor (33). Clinical studies in nephrotic syndrome determined that the endodermal glycocalyces damage marker (SDC-1) was significantly associated with 24-hour urinary protein excretion, TG, HDL-C and LDL-C levels (34). Therefore, these studies have demonstrated that ox-LDL induced the increase of SDC-1 expression in vascular endothelial cells, which was consistent with the pathological features of atherosclerosis.

Previous studies have shown that miR-19a-3p expression in endothelial cells was significantly down-regulated by LPS stimulation (35). Overexpression of miR-19a-3p protected endothelial cells from the LPS-induced apoptosis through the ASK1/p38 pathway (35). miR-19a-3p was also involved in the H_2O_2-induced autophagy injury of HUVECs (36). Our study found that overexpression of miR-19a-3p promoted cell proliferation, inhibited apoptosis, cholesterol efflux and the SDC-1, ABCA1 and ABCG1 expressions in ox-LDL-induced HAECs. The above studies proved that miR-19a-3p might be a potential target for improving atherosclerosis.

ox-LDL promoted endothelial cell angiogenesis *in vitro*, leading to plaque instability and vulnerability (37). Agomir with miR-9 or siRNA against OLR1 inhibited the p38 mitogen-activated protein kinase (p38MAPK) pathway and atherosclerotic plaque formation in mice (38). Overexpression of SDC-1 affected the secretion of angiogenic factors in mesothelioma cells, thereby inhibiting endothelial cell proliferation, tube formation and wound healing (39). We proved that overexpression of miR-19a-3p improved HAECs characterization and cholesterol efflux in the ox-LDL group. However, we did not explore the role of miR-19a-3p in atherosclerotic plaque formation in mice. This was a limitation in this study, which will be explored in future research.

SDC-1 was a receptor for triglyceride-rich lipoproteins, growth factors, chemokines, and enzymes (40). In cirrhosis, SDC-1 mainly prevented the early stages of fibrosis by enhancing the clearance of TGFβ1 and THBS1 from the circulation (41). SDC-1 also prevented hepatocellular carcinoma by interfering with several signaling pathways and enhancing cell-cycle blockade (41). In asthma, increased SDC-1 expression was correlated with TGFβ1/Smad3-mediated airway remodeling *in vivo* and *in vitro* (42,43). We found that overexpression of miR-19a-3p inhibited the expression of SDC-1, TGF-β1 and p-Smad3 proteins in ox-LDL-induced HAECs. Therefore, these studies demonstrated that overexpression of miR-19a-3p inhibited the apoptosis, SDC-1 level, cholesterol efflux and activation of the TGF-β1/Smad3 pathway in ox-LDL-induced HAECs.

Acknowledgment

This study was supported by Scientific Research Fund of Hunan Provincial Health Commission (B20182018).

Author contributions

Qiao Jin and Yiming Deng: clinical studies, experiments work, data analysis and manuscript writing. Qiao Jin and Yiming Deng contributed equally to this paper. Liang Li, Luping Jiang and Ran Chen: study concepts, research design and manuscript editing. All authors read and approved the fnal manuscript.

Conflict of interest

The authors state that there are no conflicts of interest to disclose.

Data Availability Statement

The datasets used and analyzed during the current study are available from the corresponding author on reasonable request.

Ethics approval

Ethical approval was obtained from the Ethics Committee of Nanhua University Affiliated Changsha Central Hospital (201812). All procedures have been performed in accordance with the Declaration of Helsinki. Written informed consent was signed by all participants.

References

1. Herrington W, Lacey B, Sherliker P, Armitage J, Lewington S. Epidemiology of Atherosclerosis and the Potential to Reduce the Global Burden of Atherothrombotic Disease. Circ Res. 2016; 118(4):535-546.
2. Schaftenaar F, Frodermann V, Kuiper J, Lutgens E. Atherosclerosis: the interplay between lipids and immune cells. Curr Opin Lipidol. 2016; 27(3):209-215.
3. Bäck M, Yurdagul A, Jr., Tabas I, Öörni K, Kovanen PT. Inflammation and its resolution in atherosclerosis: mediators and therapeutic opportunities. Nat Rev Cardiol. 2019;16(7):389-406.
4. Tomaniak M, Katagiri Y, Modolo R, de Silva R, Khamis RY, Bourantas CV, et al. Vulnerable plaques and patients: state-of-the-art. Eur Heart J. 2020; 41(31):2997-3004.
5. Singh S, de Ronde MWJ, Kok MGM, Beijk MA, De Winter RJ, van der Wal AC, et al. MiR-223-3p and miR-122-5p as circulating biomarkers for plaque instability. Open Heart. 2020;7(1): e001223.
6. Neth P, Nazari-Jahantigh M, Schober A, Weber C. MicroRNAs in flow-dependent vascular remodelling. Cardiovasc Res. 2013; 99(2):294-303.
7. Alexandru N, Constantin A, Nemecz M, Comariţa IK, Vîlcu A, Procopciuc A, et al. Hypertension Associated With Hyperlipidemia Induced Different MicroRNA Expression Profiles in Plasma, Platelets, and Platelet-Derived Microvesicles; Effects of Endothelial Progenitor Cell Therapy. Front Med (Lausanne). 2019; 6:280.
8. Akhtar S, Hartmann P, Karshovska E, Rinderknecht FA, Subramanian P, Gremse F, et al. Endothelial Hypoxia-Inducible Factor-1α Promotes Atherosclerosis and Monocyte Recruitment by Upregulating MicroRNA-19a. Hypertension. 2015; 66(6):1220-1226.
9. Zhang BY, Han L, Tang YF, Zhang GX, Fan XL, Zhang JJ, et al. METTL14 regulates M6A methylation-modified primary miR-19a to promote cardiovascular endothelial cell proliferation and invasion. Eur Rev Med Pharmacol Sci. 2020; 24(12):7015-7023.
10. Fang H, Li HF, He MH, Yang M, Zhang JP. HDAC3 Downre-

gulation Improves Cerebral Ischemic Injury via Regulation of the SDC1-Dependent JAK1/STAT3 Signaling Pathway Through miR-19a Upregulation. Mol Neurobiol. 2021; 58(7):3158-3174.
11. Angsana J, Chen J, Smith S, Xiao J, Wen J, Liu L, et al. Syndecan-1 modulates the motility and resolution responses of macrophages. Arterioscler Thromb Vasc Biol. 2015; 35(2):332-340.
12. Voyvodic PL, Min D, Liu R, Williams E, Chitalia V, Dunn AK, et al. Loss of syndecan-1 induces a pro-inflammatory phenotype in endothelial cells with a dysregulated response to atheroprotective flow. J Biol Chem. 2014; 289(14):9547-9559.
13. Nemoto T, Minami Y, Yamaoka-Tojo M, Kato A, Katsura A, Sato T, et al. Endothelial glycocalyx and severity and vulnerability of coronary plaque in patients with coronary artery disease. Atherosclerosis. 2020; 302:1-7.
14. Dogné S, Flamion B. Endothelial Glycocalyx Impairment in Disease: Focus on Hyaluronan Shedding. Am J Pathol. 2020; 190(4):768-780.
15. Fang R, Zhang N, Wang C, Zhao X, Liu L, Wang Y, et al. Relations between plasma ox-LDL and carotid plaque among Chinese Han ethnic group. Neurol Res. 2011; 33(5):460-466.
16. Wang Z, Guo X, Zhang Q, Du G, Zeng Z, Zheng C, et al. Elimination of Ox-LDL through the liver inhibits advanced atherosclerotic plaque progression. Int J Med Sci. 2021; 18(16):3652-3664.
17. He Z, Xue H, Liu P, Han D, Xu L, Zeng X, et al. miR-4286/TGF-β1/Smad3-Negative Feedback Loop Ameliorated Vascular Endothelial Cell Damage by Attenuating Apoptosis and Inflammatory Response. J Cardiovasc Pharmacol. 2020; 75(5):446-454.
18. Xu C, Lu G, Li Q, Zhang J, Huang Z, Gao X. Selenium modulates MMP2 expression through the TGFβ1/Smad signalling pathway in human umbilical vein endothelial cells and rabbits following lipid disturbance. J Trace Elem Med Biol. 2017; 42:59-67.
19. Liu C, Li G, Wang P, Wang Y, Pan J. Characterization of spontaneous hydrocephalus development in the young atherosclerosis-prone mice. Neuroreport. 2017; 28(16):1108-1114.
20. Song CY, Kim BC, Lee HS. Lovastatin inhibits oxidized low-density lipoprotein-induced plasminogen activator inhibitor and transforming growth factor-beta1 expression via a decrease in Ras/extracellular signal-regulated kinase activity in mesangial cells. Transl Res. 2008; 151(1):27-35.
21. Hang L, Peng Y, Xiang R, Li X, Li Z. Ox-LDL Causes Endothelial Cell Injury Through ASK1/NLRP3-Mediated Inflammasome Activation via Endoplasmic Reticulum Stress. Drug Des Devel Ther. 2020; 14:731-744.
22. Agarwal V, Bell GW, Nam JW, Bartel DP. Predicting effective microRNA target sites in mammalian mRNAs. Elife. 2015; 12:4: e05005.
23. Nair A, Margolis MP, Kuban BD, Vince DG. Automated coronary plaque characterisation with intravascular ultrasound backscatter: ex vivo validation. EuroIntervention. 2007; 3(1):113-120.
24. Fujii K, Hao H, Ohyanagi M, Masuyama T. Intracoronary imaging for detecting vulnerable plaque. Circ J. 2013; 77(3):588-595.
25. Räber L, Mintz GS, Koskinas KC, Johnson TW, Holm NR, Onuma Y, et al. Clinical use of intracoronary imaging. Part 1: guidance and optimization of coronary interventions. An expert consensus document of the European Association of Percutaneous Cardiovascular Interventions. EuroIntervention. 2018; 14(6):656-677.
26. Liu K, Xuekelati S, Zhou K, Yan Z, Yang X, Inayat A, et al. Expression Profiles of Six Atherosclerosis-Associated microRNAs That Cluster in Patients with Hyperhomocysteinemia: A Clinical Study. DNA Cell Biol. 2018; 37(3):189-198.
27. Mushenkova NV, Summerhill VI, Zhang D, Romanenko EB, Grechko AV, Orekhov AN. Current Advances in the Diagnostic Imaging of Atherosclerosis: Insights into the Pathophysiology of Vulnerable Plaque. Int J Mol Sci. 2020; 21(8):2992.
28. Leonova EI, Galzitskaya OV. Role of Syndecans in Lipid Metabolism and Human Diseases. Adv Exp Med Biol. 2015; 855:241-258.
29. Wang H, Moore S, Alavi MZ. Expression of syndecan-1 in rabbit neointima following de-endothelialization by a balloon catheter. Atherosclerosis. 1997; 131(2):141-147.
30. Freitas IA, Lima NA, Silva GBD, Jr., Castro RL, Jr., Patel P, Lima CCV, et al. Novel biomarkers in the prognosis of patients with atherosclerotic coronary artery disease. Rev Port Cardiol (Engl Ed). 2020; 39(11):667-672.
31. Zhu Z, Li J, Zhang X. Salidroside protects against ox-LDL-induced endothelial injury by enhancing autophagy mediated by SIRT1-FoxO1 pathway. BMC Complement Altern Med. 2019; 19(1):111.
32. Kattoor AJ, Kanuri SH, Mehta JL. Role of Ox-LDL and LOX-1 in Atherogenesis. Curr Med Chem. 2019; 26(9):1693-1700.
33. Tirronen A, Vuorio T, Kettunen S, Hokkanen K, Ramms B, Niskanen H, et al. Deletion of Lymphangiogenic and Angiogenic Growth Factor VEGF-D Leads to Severe Hyperlipidemia and Delayed Clearance of Chylomicron Remnants. Arterioscler Thromb Vasc Biol. 2018; 38(10):2327-2337.
34. Salmito FT, de Oliveira Neves FM, Meneses GC, de Almeida Leitão R, Martins AM, Libório AB. Glycocalyx injury in adults with nephrotic syndrome: Association with endothelial function. Clin Chim Acta. 2015; 447:55-58.
35. Jiang WL, Zhang YF, Xia QQ, Zhu J, Yu X, Fan T, et al. MicroRNA-19a regulates lipopolysaccharide-induced endothelial cell apoptosis through modulation of apoptosis signal-regulating kinase 1 expression. BMC Mol Biol. 2015; 16:11.
36. Guo Y, Yang JH, Cao SD, Gao CX, He Y, Wang Y, et al. Effect of main ingredients of Danhong Injection against oxidative stress induced autophagy injury via miR-19a/SIRT1 pathway in endothelial cells. Phytomedicine. 2021; 83:153480.
37. Yuan R, Shi W, Xin Q, Yang B, Hoi MP, Lee SM, et al. Tetramethylpyrazine and Paeoniflorin Inhibit Oxidized LDL-Induced Angiogenesis in Human Umbilical Vein Endothelial Cells via VEGF and Notch Pathways. Evid Based Complement Alternat Med. 2018;2018:3082507.
38. Yu DR, Wang T, Huang J, Fang XY, Fan HF, Yi GH, et al. MicroRNA-9 overexpression suppresses vulnerable atherosclerotic plaque and enhances vascular remodeling through negative regulation of the p38MAPK pathway via OLR1 in acute coronary syndrome. J Cell Biochem. 2020; 121(1):49-62.
39. Javadi J, Heidari-Hamedani G, Schmalzl A, Szatmári T, Metintas M, Aspenström P, et al. Syndecan-1 Overexpressing Mesothelioma Cells Inhibit Proliferation, Wound Healing, and Tube Formation of Endothelial Cells. Cancers (Basel). 2021; 13(4):655.
40. Leonova EI, Sadovnikova ES, Shaykhutdinova ER, Galzitskaya OV, Murashev AN, Solonin AS. Hepatic and Aortic Arch Expression and Serum Levels of Syndecan-1 in ApoE(-/-) Mice. Open Biochem J. 2017;11:77-93.
41. Reszegi A, Tátrai P, Regős E, Kovalszky I, Baghy K. Syndecan-1 in liver pathophysiology. Am J Physiol Cell Physiol. 2022;323(2):C289-c94.
42. Azizi Dargahlou, S., Iriti, M., Pouresmaeil, M., Goh, L. P. W. MicroRNAs and their therapeutic and biomarker properties. Cell Mol Biomed Rep 2022; doi: 10.55705/cmbr.2022.365396.1085.
43. Zhang D, Qiao XR, Cui WJ, Zhang JT, Pan Y, Liu XF, et al. Syndecan-1 Amplifies Ovalbumin-Induced Airway Remodeling by Strengthening TGFβ1/Smad3 Action. Front Immunol. 2021;12:744477.